\



Information flow between stock markets: A Koopman decomposition approach

Semba Sherehe, Huiyun Wan(万慧云), Changgui Gu(顾长贵), and Huijie Yang(杨会杰)
Citation: Chin. Phys. B, 2022, 31 (**1**): 018902. DOI: 10.1088/1674-1056/ac16c9
Journal homepage: http://cpb.iphy.ac.cn; http://iopscience.iop.org/cpb

What follows is a list of articles you may be interested in

Pyramid scheme in stock market: A kind of financial market simulation

Yong Shi(石勇), Bo Li(李博), and Guang-Le Du(杜光乐)
Chin. Phys. B, 2021, 30 (**9**): 098901. DOI: 10.1088/1674-1056/abeef3

Theoretical analyses of stock correlations affected by subprime crisis and total assets: Network properties and corresponding physical mechanisms

Shi-Zhao Zhu(朱世钊), Yu-Qing Wang(王玉青), Bing-Hong Wang(汪秉宏)
Chin. Phys. B, 2019, 28 (**10**): 108901. DOI: 10.1088/1674-1056/ab3f22

Statistics of extreme events in Chinese stock markets

Wu Gan-Hua, Qiu Lu, Mutua Stephen, Li Xin-Li, Yang Yue, Yang Hui-Jie, Jiang Yan
Chin. Phys. B, 2014, 23 (**12**): 128901. DOI: 10.1088/1674-1056/23/12/128901

A mini-review on econophysics：Comparative study of Chinese and western financial markets

Zheng Bo, Jiang Xiong-Fei, Ni Peng-Yun
Chin. Phys. B, 2014, 23 (**7**): 078903. DOI: 10.1088/1674-1056/23/7/078903

Measuring causality by directional symbolic mutual information approach

Chen Gui, Xie Lei, Chu Jian
Chin. Phys. B, 2013, 22 (**3**): 038902. DOI: 10.1088/1674-1056/22/3/038902

Information flow between stock markets: A Koopman decomposition approach

Semba Sherehe[1,2], Huiyun Wan(万慧云)[1], Changgui Gu(顾长贵)[1], and Huijie Yang(杨会杰)[1,†]

[1] *Department of Systems Science, University of Shanghai for Science and Technology, Shanghai* 200093, *China*
[2] *Faculty of Science, Dar es Salaam University College of Education, University of Dar es Salaam, Dar es Salaam, Tanzania*

(Received 14 May 2021; revised manuscript received 10 July 2021; accepted manuscript online 22 July 2021)

Stock markets in the world are linked by complicated and dynamical relationships into a temporal network. Extensive works have provided us with rich findings from the topological properties and their evolutionary trajectories, but the underlying dynamical mechanism is still not in order. In the present work, we proposed a technical scheme to reveal the dynamical law from the temporal network. The index records for the global stock markets form a multivariate time series. One separates the series into segments and calculates the information flows between the markets, resulting in a temporal market network representing the state and its evolution. Then the technique of the Koopman decomposition operator is adopted to find the law stored in the information flows. The results show that the stock market system has a high flexibility, *i.e.*, it jumps easily between different states. The information flows mainly from high to low volatility stock markets. And the dynamical process of information flow is composed of many dynamic modes distribute homogenously in a wide range of periods from one month to several ten years, but there exist only nine modes dominating the macroscopic patterns.

Keywords: transfer entropy, Koopman operator, stock markets

PACS: 89.65.Gh, 05.45.Tp, 89.75.Fb, 02.10.Ox **DOI:** 10.1088/1674-1056/ac16c9

1. Introduction

The stock markets distributed over the world are networked by complicated and dynamical relationships into a global system. The relations are integration results of the natural disasters, the social/political/armed conflicts, and the flow of capitals. The environmental factors cover a wide time scale from several days, such as the Suez Canal Blockage[1] to several months or even more than one year, such as the novel COVID-19 pandemic.[2–5] And the flow of capitals also has a rich pattern composing of the strategic, tactical, and speculative investments from different institutions. The stock market network attracts persistent attentions of researchers from diverse fields for its potential use in theory and practice.

The relationships between stock markets are currently detected through the cross-correlation,[6,7] the causality inference,[8] and the information flow.[9] For instance, to detect the influence stored in cross-correlations, the concept of time delay stability is designed.[10–14] The influence is realized by a successive physical process of sending signals from the influencer, receiving signals by the influenced one and its responses. The signals may be different completely, but the delay time from the sending to the response is determined by the intrinsic properties of the systems and keeps unchanged. One calculates the cross-correlation coefficients between the output series for different delays and finds the specific delay at which the absolute value of the cross-correlation coefficient reaches the maximum, called time delay for the cross-correlation.[15] The value of the cross-correlation and the time delay stability are used cooperatively to identify the influence. The Granger causality[16] of one market, for another example, implies that the history of the causal market has a significant ability to explain the present state of the explained market, which is evaluated by regressions of the structural equations.[17,18]

The couplings between the stock markets induce to and can be represented subsequently with information flows, measured by various entropy quantifiers.[19–26] The present state of one market depends strongly on its history. Using a specified number of historical records as a condition, one can obtain the conditional probabilities and the conditional entropy.[27] Adding the historical recordings for another stock market to the condition, the conditional entropy will become smaller due to the newly introduced information. The decreasing quantity is called transfer entropy.[28] A higher value of transfer entropy implies that the added stock market has a significant explanation ability.[28–31]

The index records for the stock markets form a multivariate time series. One separates the time series into segments with a specified length (*e.g.*, one year) and reconstructs their corresponding stock market networks, all of which will form a temporal network.[31] The structural and evolutionary behaviors are then displayed using the curves of structural properties for the snapshot networks versus time. Fruitful findings have

†Corresponding author. E-mail: hjyang@ustc.edu.cn

© 2022 Chinese Physical Society and IOP Publishing Ltd

been reported in recent years.[32–34] For instance, the mutual entropy between successive networks for a total of 57 industry portfolios in the American stock market reaches peaks at financial crises.[17] According to the signs of components for the eigenvectors corresponding to several largest eigenvalues of stock networks, one can separate the stocks into reasonable groups consistent with that in reality.[35] And the average transfer entropy for the market network reaches peaks several months before each financial crisis.[31] But the evolutionary mechanism underlying the temporal network is still not in order.

Recent years have witnessed a rapid development of dynamic mode decomposition (DMD).[36–40] It is built on the idea of Koopman operator approximation, *i.e.*, though the evolutionary process of a system is generally nonlinear, in each time step it can be mimicked by a linear one, and in a short time duration the system obeys the same law. Many works have shown its powerfulness in discovering the underlying mechanism from experimental records. It is widely used in the identification and monitoring of mobile objects, displaying the complicated dynamical patterns in turbulent fluids, diagnostics and predictions.[41]

The present work proposes a scheme that reveals underlying dynamical law stored in the information flows between stock markets. First, we collect the monthly closing price series for many stock markets and calculate the corresponding volatility series. The volatility series are separated into segments with a specified length each. For each segment, we calculate the transfer entropies between all the markets, forming a weighted-directional information flow network used to represent the local state of the system in the corresponding time duration. The successive weighted-directional information flow networks make the dynamical process of information flow. Then the Koopman operator is adopted to model this dynamical process with eigenfunctions. The model gives the dynamical law for the entropy flow in the global stock market system. The generated dynamic model displays rich evolution patterns, *e.g.*, the non-normal energy growth indicating the stock market system jumps easily between different states (called flexibility of stock market system). Also, the information flows mainly from high volatility stock markets to low volatility stock markets.

The materials and methodologies are introduced in detail in Section 2. In Section 3 we present the numerical experiments and observations. Summaries and conclusions are provided in Section 4.

2. Materials and methodologies

Figure 1 illustrates the methodology framework.

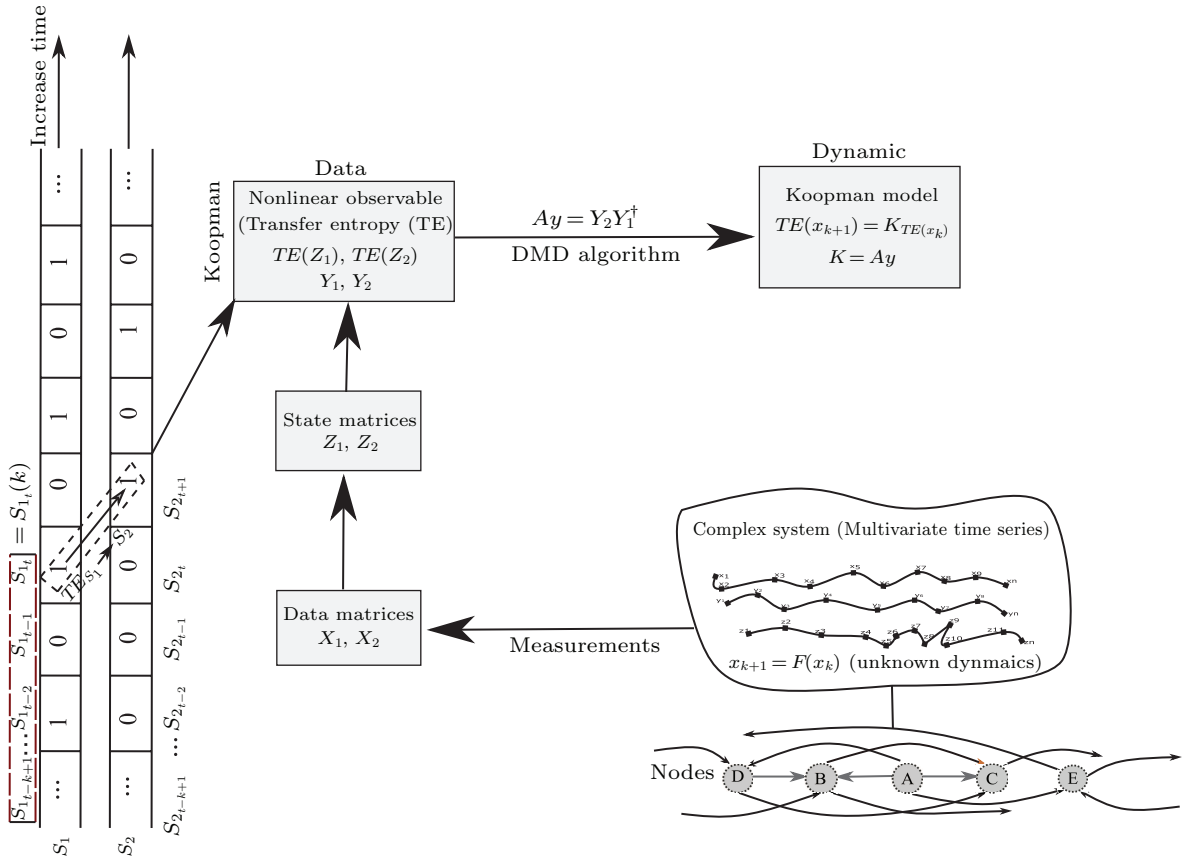


Fig. 1. The methodology framework: The framework shows how the complex systems with the unknown governing equation and nonlinear produce the multivariate time series data, used to generate the dynamical information model by deploying transfer entropy integrated Koopman mode decomposition.

2.1. Data

We collected the monthly closing prices for a total of 22 stock markets from June 1, 2002, to January 1, 2021. The stock markets distribute over five continents including, South America, North America, Asia, Europe, Australia, and Africa, as listed in Table 1. From each continent, we have chosen at least one market. The data can be downloaded freely from the website finance.yahoo.com.

Table 1. The list of stock indices.

ID	INDEX	Economy	ID	INDEX	Economy
1	AEX	Netherland	12	NASDQ	USA
2	BSESN	India	13	NICKEL	Canada
3	BVSP	Brazil	14	NYA	USA
4	CAC40	France	15	SSE	China
5	CRUDE OIL	USA	16	S&P100	USA
6	DAX	German	17	SZIAX	USA
7	DJ	USA	18	TSX	Canada
8	FHI	Egypt	19	TWI	USA
9	GOLD	USA	20	XAX	USA
10	HSI	Hong Kong	21	FTSE100	UK
11	MSM	Oman	22	AORD	Austrilia

Let us denote the records for the closing prices with

$$P=\begin{Bmatrix} P_{1,1} & P_{1,2} & P_{1,3} & \cdots & P_{1,T} \\ P_{2,1} & P_{2,2} & P_{2,3} & \cdots & P_{2,T} \\ P_{3,1} & P_{3,2} & P_{3,3} & \cdots & P_{3,T} \\ \vdots & \vdots & \vdots & \ddots & \vdots \\ P_{I,1} & P_{I,2} & P_{I,3} & \cdots & P_{I,T} \end{Bmatrix},$$

where $P_{i,t}$ means the closing price of the i-th stock index at the t-th trading month, $T=224$ is the total number of the records for each stock market, and $I=22$ is the total number of the stock markets. Adopting the price volatility definition given by

$$x_{i,t}\equiv|\ln(P_{i,t})-\ln(P_{i,t-1})|,$$

the closing prices are converted to a multivariate series with totally 22 variables and a length of 223 (depicted also in Fig. 2(a1)),

$$X=\begin{Bmatrix} x_{1,1} & x_{1,2} & x_{1,3} & \cdots & x_{1,223} \\ x_{2,1} & x_{2,2} & x_{2,3} & \cdots & x_{2,223} \\ x_{3,1} & x_{3,2} & x_{3,3} & \cdots & x_{3,223} \\ \vdots & \vdots & \vdots & \ddots & \vdots \\ x_{22,1} & x_{22,2} & x_{22,3} & \cdots & x_{22,223} \end{Bmatrix}. \tag{1}$$

Let a window with a specified length $w=24$ months (two years) slide along the volatility series X with a step of one month, resulting into a total of $T-w+1=200$ segments X_k, $k=1,2,\ldots,200$. The k-th segment reads

$$X_k=\begin{Bmatrix} x_{1,\,k} & x_{1,\,k+1} & x_{1,\,k+2} & \cdots & x_{1,\,k+w-1} \\ x_{2,\,k} & x_{2,\,k+1} & x_{2,\,k+2} & \cdots & x_{2,\,k+w-1} \\ x_{3,\,k} & x_{3,\,k+1} & x_{3,\,k+2} & \cdots & x_{3,\,k+w-1} \\ \vdots & \vdots & \vdots & \ddots & \vdots \\ x_{22,\,k} & x_{22,\,k+1} & x_{22,\,k+2} & \cdots & x_{22,\,k+w-1} \end{Bmatrix}. \tag{2}$$

The transfer entropy is adopted to measure the information flows between stock markets. To calculate the transfer entropy, one has to estimate the conditional probabilities from the initial volatility series. It requires a large number of volatilities, specifically when there exists a long-term memory. The volatility series segments are coarse-grained first, respectively, to make the calculations reliable. From X_k one extracts the segment corresponding to the i-th stock market, *i.e.*, $X_{i,k}=\{x_{i,k},x_{i,k+1},\ldots,x_{i,k+w-1}\}$, divides the range from the minimum to the maximum into four bins with identical width, denoted with identification numbers 0, 1, 2, and 3. Replacing all the elements in $X_{i,k}$ with the identification numbers of the bins they fall in, resulting in a new series of volatility catalogues. The labels 0, 1, 2, and 3 respectively denote extremely low, low, high and very high volatilities. The procedure on the whole X_k converts the segment of volatility series to a coarse-grained one,

$$S_k=\begin{Bmatrix} s_{1,\,k} & s_{1,\,k+1} & s_{1,\,k+2} & \cdots & s_{1,\,k+w-1} \\ s_{2,\,k} & s_{2,\,k+1} & s_{2,\,k+2} & \cdots & s_{2,\,k+w-1} \\ s_{3,\,k} & s_{3,\,k+1} & s_{3,\,k+2} & \cdots & s_{3,\,k+w-1} \\ \vdots & \vdots & \vdots & \ddots & \vdots \\ s_{22,\,k} & s_{22,\,k+1} & s_{22,\,k+2} & \cdots & s_{22,\,k+w-1} \end{Bmatrix}. \tag{3}$$

Hereafter, we will use S_k, $k=1,2,\ldots,200$ to calculate the information flows.

2.2. Temporal information flow network

As an illustration, let us calculate the transfer entropy from the m-th stock market to the n-th stock market in the k-th time duration. The corresponding series read

$$\begin{aligned} S_{m,k}&=\{s_{m,k},s_{m,k+1},\ldots,s_{m,k+w-1}\},\\ S_{n,k}&=\{s_{n,k},s_{n,k+1},\ldots,s_{n,k+w-1}\}, \end{aligned} \tag{4}$$

from which one estimates the conditional probabilities $p(\alpha|\beta)\equiv p(s_{n,k+1}=\alpha|s_{n,k}=\beta)$ and $p(\alpha|\beta,\gamma)\equiv p(s_{n,k+1}=\alpha|s_{n,k}=\beta,s_{m,k}=\gamma)$, α, β, $\gamma=0$, 1, 2, 3, giving us the one-step memory effect in $S_{n,k}$, and the influence of the present state of the m-th and n-th stock markets on the next state of the n-th stock market, respectively. The transfer entropy is defined to be the difference between the corresponding two conditional entropies,

$$\begin{aligned} &TE^k(m\to n)\\ &=-\sum_{\alpha,\beta=0,1,2,3}p(\alpha|\beta)\ln[p(\alpha|\beta)]\\ &\quad+\sum_{\alpha,\beta,\gamma=0,1,2,3}p(\alpha|\beta,\gamma)\ln[p(\alpha|\beta,\gamma)]. \end{aligned} \tag{5}$$

The transfer entropies between all the stock markets in the k-th series segment form a transfer entropy matrix, TE^k, a 22×22

matrix whose entity TE^k $(m \to n)$ is the transfer entropy from the m-th stock market to the n-th stock market. The dynamical process for information flows between stock markets is the matrix series, $TE = \{TE^k,\ k = 1,2,\ldots,200\}$, called temporal information flow network.

Note that we consider only the one-step memory in the series, while in reality, there exist long-term memories. The one-step memory gives us with the immediate influence, which may display the influences much more clearly. If we consider the long-term memories, there will appear complicated relationships due to the multi-step responses between stock markets. The direct influences may be merged in the complicated responses.

2.3. Koopman mode decomposition

Now we rewrite the dynamical process for the information flows TE with a matrix with 22×22 rows and 200 columns, denoted with Y, whose entities read

$$\begin{aligned} &Y(22*(i-1)+j,k) = TE^k(i,j),\\ &i,j = 1,2,\ldots,22, \quad k = 1,2,\ldots,200. \end{aligned} \tag{6}$$

In this procedure, the information flows in the segments are re-arranged into 22×22-rows vectors, respectively.

Assuming the transition from the present information flow matrix to the successive next one can be mimicked by using a linear relation $\mathcal{K}$, we have

$$\begin{aligned} &[Y(:,2), Y(:,3), \ldots, Y(:,200)]\\ &\approx \mathcal{K}[Y(:,1), Y(:,2), \ldots, Y(:,199)], \end{aligned} \tag{7}$$

denoted with $Y_2 = \mathcal{K}Y_1$, where $Y(:,k)$ refers to the k-th column in Y, *i.e.*, the information flows between stock markets in the k-th segment (time duration). The matrix $\mathcal{K}$ is called Koopman operator, satisfying the following equation:

$$\mathcal{K} = Y_2 Y_1^{\dagger}, \tag{8}$$

where $Y_1^{\dagger}$ denotes the Moore–Penrose pseudoinverse[42,43] of Y_1. It is currently estimated by minimizing the error

$$||Y_2 - \mathcal{K}Y_1||_F \equiv ||Y^{\text{error}}||_F,$$

i.e., the Frobenius norm of Y^{error}, $\sqrt{\sum_{i=1}^{p}\sum_{j=1}^{q}|Y_{ij}^{\text{error}}|^2}$.

The dynamic modes correspond to the eigenfunctions of $\mathcal{K}$. The operator $\mathcal{K}$ is a matrix with a size of 484×484, implying that we have a total of 484 eigenvalues and corresponding eigenfunctions. In reality, most of the eigenfunctions reflect the microscopic details depending on the noises and occasional events. Herein, we are interested in the eigenfunctions that can give us the intrinsic law in the information flows.

Technically, the singular value decomposition (SVD) is used. We compute the reduced and appropriately truncated SVD of Y_1, $Y_1 \approx U_r \Sigma_r V_r^*$, where r refers to the reduced rank of the approximated operator less than $\min(22 \cdot 22, 199) = 199$. In most cases the intrinsic dynamical law can be captured by selecting a small value of r. A low-rank approximation of $\mathcal{K}$ is then defined to be $\tilde{\mathcal{K}} = \tilde{\mathcal{K}} = U_r^* \mathcal{K} U_r = U_r^* Y_2 V_r \Sigma_r^{-1}$, whose eigendecomposition reads

$$\tilde{\mathcal{K}} W = W\Lambda, \quad \Lambda = \text{diag}(\lambda_1, \lambda_2, \lambda_3, \ldots, \lambda_r), \tag{9}$$

where the columns of $W \in \mathbb{C}^{r\times r}$ and the diagonal entries of $\Lambda \in \mathbb{C}^{r\times r}$ are the eigenfunction (eigen-information) and the eigenvalues of $\tilde{\mathcal{K}}$, respectively. The eigenfunction (eigen-information) of $\mathcal{K}$ corresponding to the λ_i is

$$\phi_i = Y_2 V \Sigma^{-1} w_i, \tag{10}$$

where w_i is the i-th column of W. Approximating the snapshot y_i with $\mathcal{K}y_{i-1}$, we reach a coupled spatial-temporal model

$$\hat{y}(t) = \mathcal{K}^t y_0 = \Phi \Lambda^t \boldsymbol{b}, \tag{11}$$

where $\Phi \in \mathbb{C}^{n\times r}$ consists of the columns of ϕ_i, and $\boldsymbol{b}$ is a set of weights satisfying $y_0 = \Phi \boldsymbol{b}$.

3. Experimental results and observations

Figure 2(a1) shows the volatility series for all the stock markets. The FHI stock market in the Egypt economy area (ID = 8) has higher volatilities than others. The flow process is not random, *i.e.*, there exist spatial patterns evolving slowly along time, as shown in the heat-map for constructed information flow process in panel (a2). In panel (b1) the singular values of Y_1 is ranked in descending order. The ranked singular value turns out to decrease faster than an exponential law. Actually, the first nine of the square singular values dominate up to 93% of the sum of all the square singular values (see panel (b2)). The most dominant one contributes 75%, reflecting the clear demarcation of the information flows between and within the stock indices. The eigenvalues for the nine dominant modes read

$$\lambda = \{0.9047 \pm 0.111\text{i},\ 0.9935,\ 0.8823,\ 0.9182 \pm 0.0444\text{i},\ 0.9563 \pm 0.0074\text{i},\ 0.9347\},$$

which are obtained by using the Koopman mode decomposition after truncation of the singular values. Because the step in our calculation is one month, the corresponding periods for these modes are $\geq 1/0.111 \sim 9$ months.

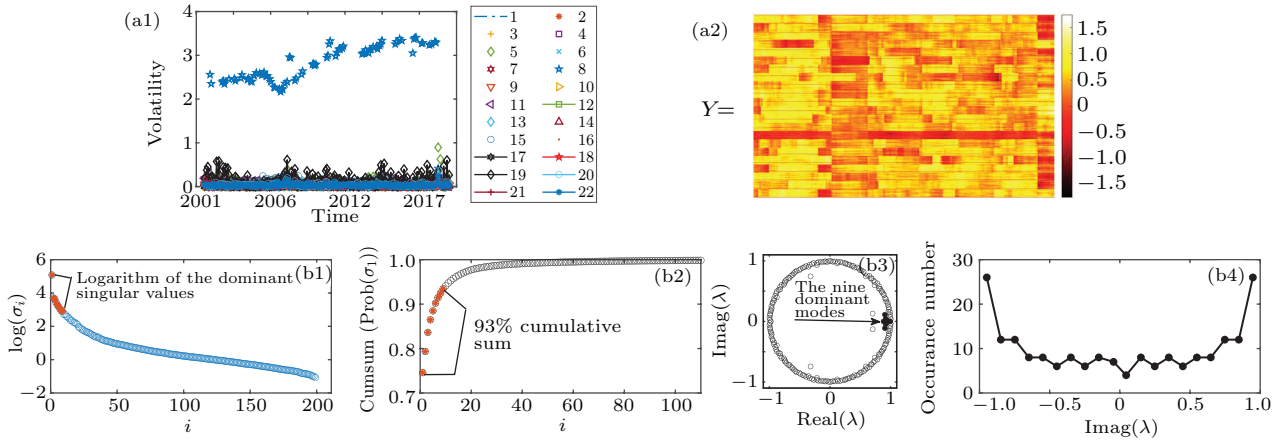


Fig. 2. (a1) The monthly volatilities for the 22 stock markets in Table 1, (a2) the heat map of the temporal information flow of Y, (b1) the logarithm of the singular values. (b2) The cumulative sum of the probability of the square singular values. The top nine dominate up to 93% of the sum of all the square singular values, called dominant modes. (b3) The eigenvalues of $\mathcal{K}$, in which the dominant modes are marked with solid circles. (b4) The distribution of the imaginary parts of the eigenvalues of $\mathcal{K}$.

From Eq. (11) one can find that the specific characteristics for each component are determined by three factors, including the amplitude stored in Φ, the period determined by the imaginary part of the eigenvalue stored in Λ, and the decaying speed determined by the real part of the eigenvalue stored in Λ. Hence, the modes whose eigenvalues have small or even zero imaginary parts and positive real parts determine the macroscopic behavior of the information flows. The modes whose eigenvalues have large imaginary parts or negative real parts reflect the microscopic behaviors of the information flows or simply the noises, because a large imaginary part implies a rapid oscillation and a negative real part an odd–even oscillation with a period of one month. In panel (b3) we display all the 199 eigenvalues of $\mathcal{K}$ (open circles), in which those corresponding to the nine dominant modes are marked with solid circles. The eigenvalues distribute mainly on a circle with several exceptions, and are symmetrical with respect to the level line $\mathrm{imag}(\lambda) = 0$. The real parts of the eigenvalues are all less than one, *i.e.*, the system is stable. The dominant modes have smaller or even zero imaginary parts and large real parts, corresponding to the macroscopic behaviors of the information flows. From the distribution of the imaginary parts for the 199 eigenvalues (panel (b4)) one can find that besides the nine dominant modes around the zero point of imaginary part, the modes distribute homogenously in the wide range of $(-0.7, +0.7)$, *i.e.*, the corresponding modes cover a wide range of periods from about one month to more than twenty years, without a characteristic period. The ignorable contributions for the modes can be explained by the small or negative values of the corresponding real parts.

The dynamical model is finally constructed as

$$\hat{Y}(t) = \left[\phi(:,1) * \lambda_1^t, \phi(:,2) * \lambda_2^t, \ldots, \phi(:,9)_1 * \lambda_9^t\right] * \boldsymbol{b}. \quad (12)$$

Generally speaking, the system shows a damping behavior. As shown in Fig. 3(a), the eigen-information flows between 154–176 modes are significantly higher than that between others, *i.e.*, there exist strong-directional information flows from the indices with high volatilities to that with low volatilities. Also, the eigen-information reflects the exact-true information flows because in each segment, there is no information flow within the same stock indices.

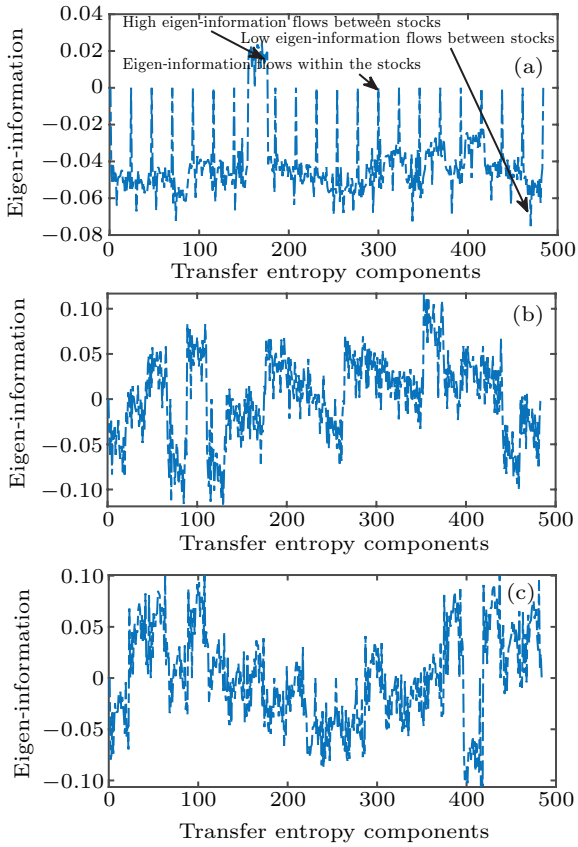


Fig. 3. The three most dominant eigenfunctions (eigen-information) of $Y1$. (a) Reflect the exact-true information flows because, in each segment, it has no information flows (quantified as 0) within the same stock indices. The other two (shown in panels (b) and (c)) do not show a clear demarcation between and within the stock indices since they have no information flows between the stock indices.

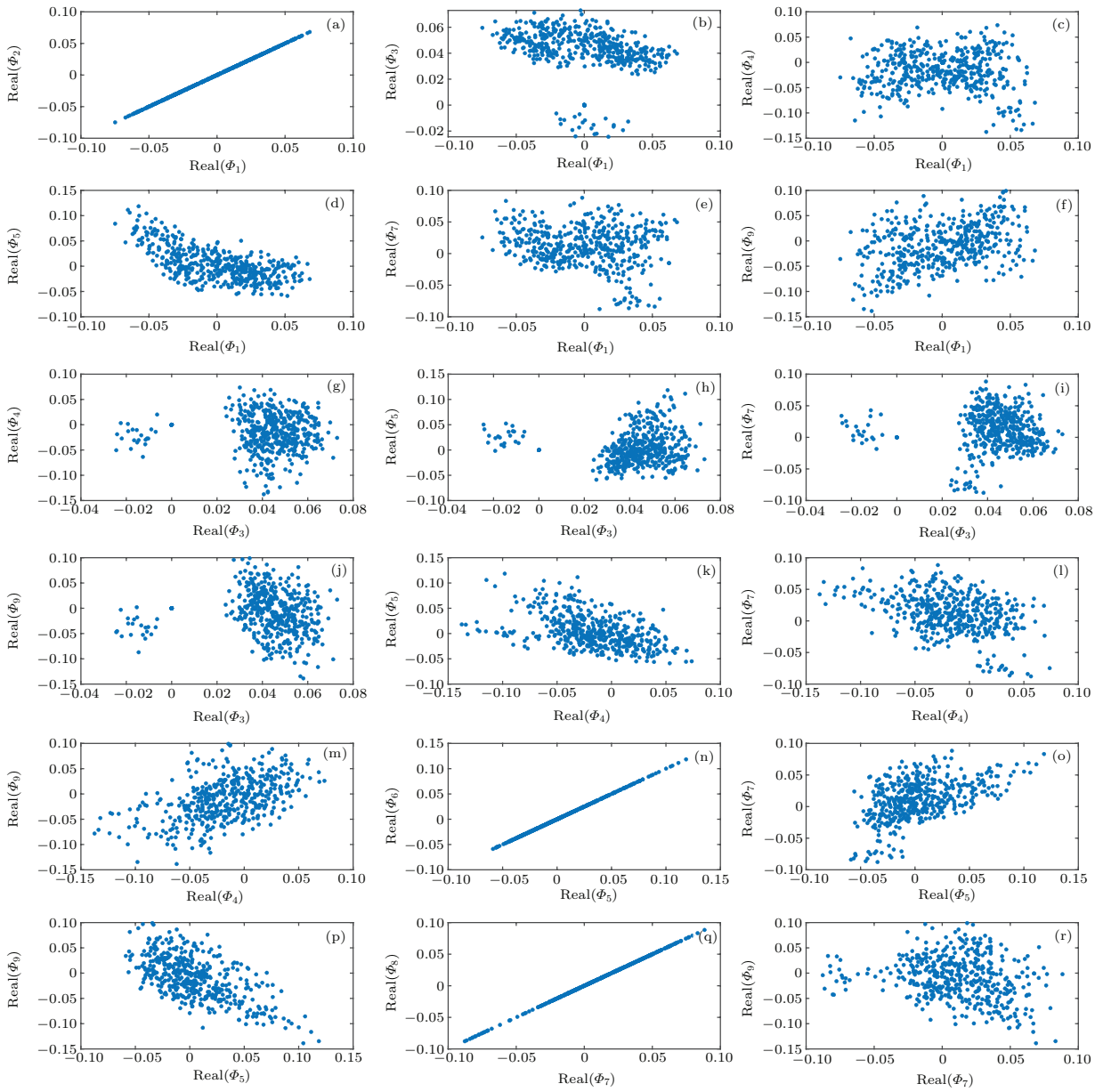


Fig. 4. Correlations between the eigenfunctions: The distributions of the Koopman decomposition modes are not orthonormal. They are no significant linear correlation, between most of the eigenfunctions. Panels (a), (n), and (q) display the strong correlations between the eigenfunctions with its conjugate.

Figure 4 shows the relations between the 9 eigenfunctions. The correlations between the eigenfunction pairs numbered $\{1,2\}$, $\{5,6\}$, and $\{7,8\}$ each are strong, actually their cross-correlation coefficients are all $+1$, as shown in the panels (a), (n), and (q). The two eigenfunctions in each pair correspond to two eigenvalues conjugating each other. The correlations between the other eigenfunctions are very weak. The Koopman mode decomposition produces non-orthonormal eigenfunctions.

The transfer entropy eigenfunctions (eigen-informations) are presented in Figs. 5(a1)–5(f1), where each 484-row eigenfunction vector is recovered to a 22×22 matrix. The directional information flows are also displayed with the networks in the panels (a2)–(f2). The broader a link, the stronger influence between the linked stock indices. For visual convenience, we filter out the weak flows less than 0.05. The panels (a3)–(f3) are the distributions of the information flows in the panels (a1)–(f1). Most of the dynamic information flows in panel (c1) are less than 0.05, resulting in the sparse directional linkages in panel (c2). And they distribute randomly (panel (c3)). Its corresponding eigenvalue is 0.8823 (the least one). In panel (b1), most of the dynamic information flow values are greater or equal to 0.05, leading to a densely connected network (panel (b2)), implying the clear demarcation information flows between and within the stock indices. The corresponding eigenvalue is 0.9935 (the largest one). The FHI with ID = 8 has no in-flow information, while the information from this stock index flows out to all the 21 stock indices. The information flows between the remaining 21 are bidirectional (panels (b2) and (b3)). The most stronger influences occur on the linkages FHI→S&P100(8,16), TWI→NASDQ(19,12), FHI→NICKEL(8,13), and FHI→NASDQ(8,12) (panel (b1)).

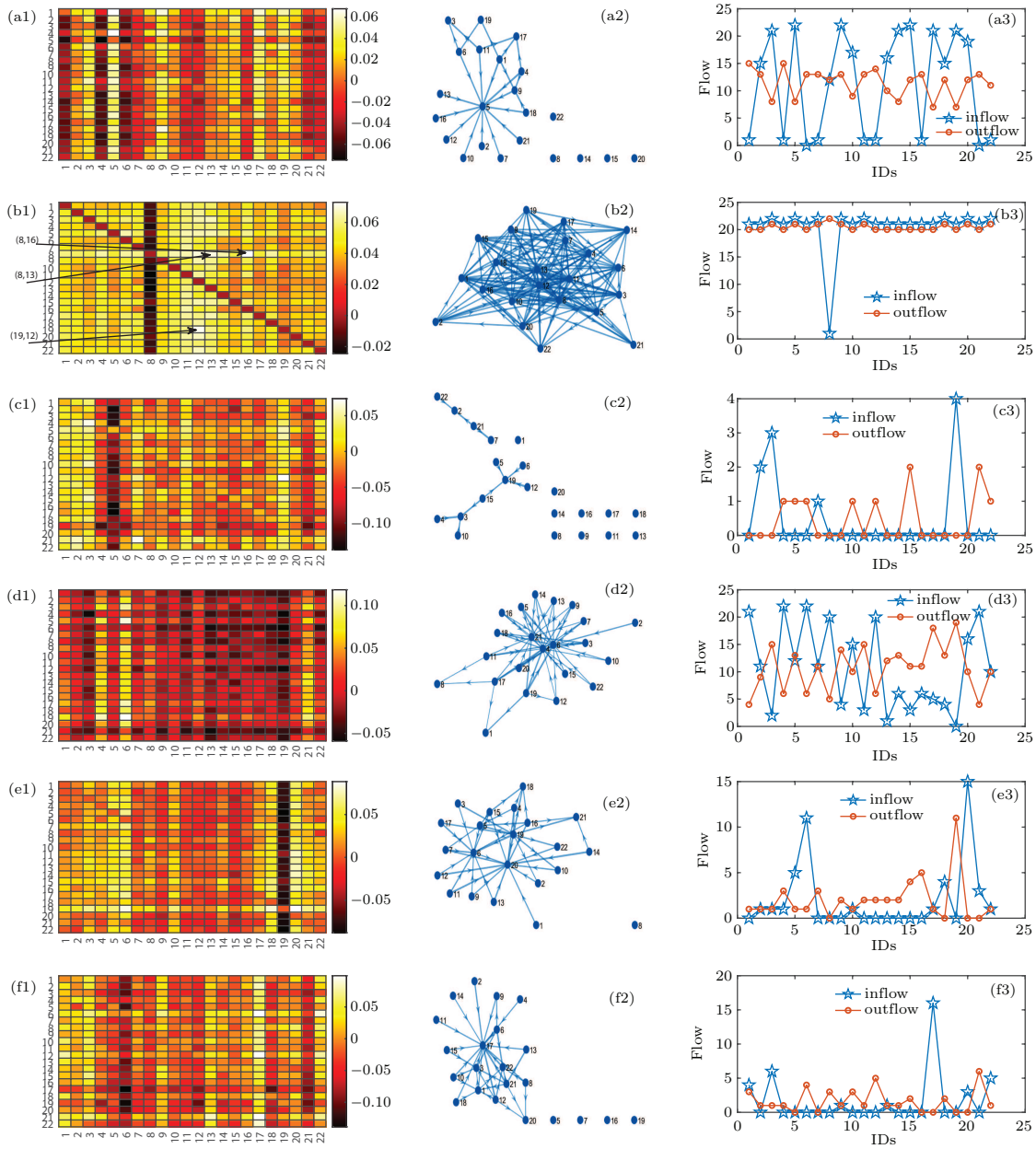


Fig. 5. Eigenfunctions: (a1)–(f1) the underlying information flows, which are displayed also with networks in panels (a2)–(f2). In the networks for which the weak information flows less than 0.05 are filtered out for visual convenience. Panels (a3)–(f3) are information flow distributions. Panels (a1)–(a3), (b1)–(b3), and (f1)–(f3) correspond to the eigenvalues of 0.9047 ± 0.111i, 0.9935, 0.8823, 0.9182 ± 0.0444i, 0.9563 ± 0.0074i, and 0.9347, respectively.

Table 2. Real modes power ($P_i = \langle \phi_i, \phi_i \rangle_2 = ||\phi_i||_2^2$), and numbers for information flows, and mono-directional information flows.

Modes power	0.9871	0.8780	0.7870
In/outflows	441	194	157
Mono-direction flows	1	12	16

As shown in Table 2, the increase of mode power implies the increase of double-directional information flow, but the mono-direction flow increases with the decreasing power. When the mode power is 0.9871 the mono-directional stock is FHI, and the bi-directional stocks are AEX, BSESN, BVSP, CAC40, CRUDE OIL, DAX, DJ, GOLD, HSI, MSM, NASDQ, NICKEL, NYA, SSE, S&P100, SZIAX, TSX, TWI, XAX, FTSE, AORD. For 0.8780 mode power, the mono-directional stocks are CAC40, CRUDE OIL, DAX, FHI, HSI, MSM, NASDQ, SSE, SZIAX, TSX, TWI, and FTSE, and bi-directional are stocks AEX, BSESN, BVSP, DJ, GOLD, NICKEL, NYA, S&P100, XAX, and AORD. For 0.7870 mode power, the mono-directional stocks are CAC40, CRUDE OIL, DAX, FHI, GOLD, HSI, NASDQ, NICKEL, NYA, SSE, S&P100, SZIAX, TSX, TWI, XAX, and FTSE, and bi-directional are stocks AEX, BSESN, BVSP, DJ, MSM, and AORD. For all real power modes, FHI is mono-directional, and the bi-directional are stocks AEX, BSESN, BVSP, and DJ.

In Fig. 6, the panels (a1)–(b1) present the dynamic information flows obtained with the original definition of transfer entropy and their average. In panels (a2)–(b2) the dynamic

information flows reconstructed from the Koopman mode decompositions and their average are shown, respectively. Initially the system grows then decays to the equilibrium points (see panel (b2)). This behavior in physics, specifically in fluid dynamics, is commonly known as transient energy growth-decay,[44] occurring when the eigenvalues are very close with or equal to each other with the corresponding nearly parallel eigenvectors.[45,46] The constructed model's transient energy growth–decay property is consistent with the presence of secular term ($t\exp(\omega t)$) in the dynamic system. Hence, the dynamic model for the stock market system can be approximated with

$$Z = \begin{bmatrix} \exp(\omega_1 t) & t\exp(\omega_1 t) & \frac{1}{2}t^2\exp(\omega_1 t) & \dots \\ 0 & \exp(\omega_2 t) & t\exp(\omega_2 t) & \dots \\ 0 & 0 & \exp(\omega_3 t) & \dots \\ \vdots & \vdots & \ddots & \dots \end{bmatrix},$$

where $\omega_1 \approx \omega_2 \approx \omega_3 \approx \cdots$. The Koopman operator approximately reads

$$\mathcal{K} = \begin{bmatrix} \omega_1 & u_1 & u_2 & \cdots \\ 0 & \omega_2 & u_3 & \cdots \\ 0 & 0 & \omega_3 & \cdots \\ \vdots & \vdots & \ddots & \cdots \end{bmatrix},$$

which can be truncated to a reasonable finite-dimensional with small error, *i.e.*,

$$||Y2 - \mathcal{K}Y1|| \approx \varepsilon.$$

Finally we reached a one decimal approximate Koopman operator

$$\mathcal{K} = \begin{bmatrix} 1.0 & 0 & 0 & 0 & -0 & 0.1 & -0 & -0 & -0.1 \\ -0 & 1.0 & 0 & 0.1 & -0 & 0.1 & -0 & 0 & -0 \\ 0 & -0 & 1.0 & 0 & -0 & 0 & -0 & 0.1 & 0 \\ -0 & -0 & -0 & 0.9 & -0 & -0 & 0 & 0 & 0 \\ 0 & -0 & 0 & 0 & 0.9 & 0 & 0 & -0 & -0 \\ -0 & -0 & 0 & 0 & 0 & 0.9 & 0 & 0.1 & 0 \\ 0 & 0 & 0 & -0 & 0 & 0 & 0.9 & -0 & 0 \\ 0 & 0 & -0 & -0 & 0 & -0 & 0 & 0.9 & -0 \\ 0 & 0 & 0 & 0 & 0 & -0 & 0 & 0.1 & 0.9 \end{bmatrix}. \quad (13)$$

The eigenvalues for this Koopman operator read 1, 1, 1, 0.9, 0.9, 0.9, 0.9, 0.9, 0.9, *i.e.*, they are very close with each other, implying that the eigenfunctions parallel with each other. In the field of of complex fluid, the concept of flexibility is currently used to describe the frequently and almost freely transitions of a macro-molecule between different geometrical configurations (shapes) due to the small energy gaps between the states. Accordingly, the fact of ease transitions between stock market states is defined herein to be flexibility of the stock market system.

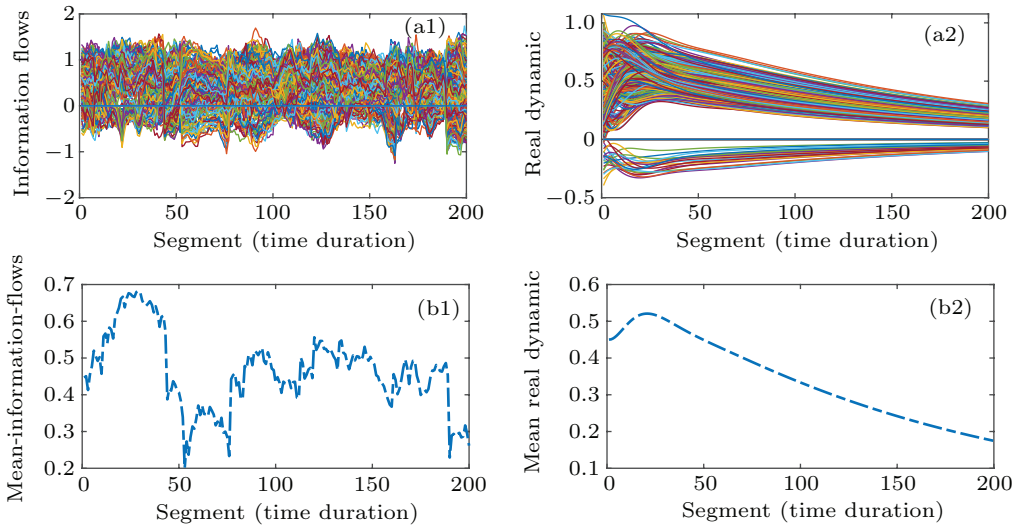


Fig. 6. (a1) The information flows obtained with the transfer entropy definition and their average (b1). (a2) The information flows reconstructed with the Koopman decompositions and their average (b2).

4. Conclusion

In this article, a novel scheme for revealing the dynamic law from the temporal network proposed. It is illustrated by using monthly volatility series for 22 stock market indices distributed over the whole world. Let a window covering two years slide along the multivariate volatility series with a step of one month to extract the segments. The segments are coarse-grained by mapping the volatilities into very low, low, high, and very high catalogues, denoted with 0 to 3, respectively. The transfer entropy is adopted to construct the information flows between all the stock markets within the segments, forming a temporal information flow network. The Koopman operator is then used to extract the evolutionary law of the entropy flows between the stock indices.

It is found that the stocks with higher levels of volatilities send information to those with lower levels of volatilities,

i.e., the influences are asymmetrical in the stock market system. The dynamic modes distribute homogenously in a wide range of periods from one month to more than twenty years. However, there exist only nine modes whose eigenvalues have large positive real parts and small or even zero imaginary parts, dominating the macroscopic patterns of the information flows. Generally speaking, there are no significant linear correlations between the eigenfunction, except between the eigenfunctions whose eigenvalues are conjugating with each other. The eigenvalues of the Koopman operator turn out to be nearly equal, and the corresponding eigenfunctions are parallel with each other, which imply high flexibility of the stock market system. And the real parts of the eigenvalues are less than one, indicating that the system is stable.

We hope the reconstructed model (Koopman operator) can find its application in prediction, intervention, and even control of the stock market system's evolution. The proposed scheme can also be extended straightly to find the evolutionary law in systems composing of multi-subsystems each, such as in the physiological system of a human body.

Acknowledgements

Project supported by the National Nature Science Foundation of China (Grant Nos. 11875042 and 11505114), the Orientational Scholar Program Sponsored by the Shanghai Education Commission, China (Grant Nos. D-USST02 and QD2015016), and the Shanghai Project for Construction of Top Disciplines, China (Grant No. USST-SYS-01).

References

[1] Alfadhli M S, Alali M S and Alkulaib H A 2021 *IOSR-JBM* **23** 64
[2] Velavan T P and Meyer C G 2020 *Trop. Med. Int. Health* **25** 278
[3] Baker S R, Bloom N, Davis S J, Kost K, Sammon M and Viratyosin T 2020 *The Rev. Asset Pric. Stud.* **10** 742
[4] Ramelli S and Wagner A 2020 *Mitigating the COVID Economic Crisis: Act Fast and Do Whatever It Takes* (Centre for Economic Policy Research, CEPR) p. 63
[5] Mazur M, Dang M and Vega M 2021 *Financ. Res. Lett.* **38** 101690
[6] Yan Y, Liu M X, Zhu X W, and Chen X S 2012 *Chin. Phys. Lett.* **29** 028901
[7] Zhao L, Wang G J, Wang M, Bao W, Li W and Stanley H E 2018 *Physica A* **506** 1104
[8] Barrett A B, Barnett L and Seth A K 2010 *Phys. Rev. E* **81** 041907
[9] He J and Shang P 2017 *Physica A* **482** 772
[10] Sun Y F and Wang C Y 2018 *Acta Phys. Sin.* **67** 148901 (in Chinese)
[11] Bashan A, Bartsch R P, Kantelhardt J W, Havlin S and Ivanov P C 2012 *Nat. Commun.* **3** 702
[12] Bartsch R P, Liu K K, Bashan A and Ivanov P C 2015 *PloS One* **10** e0142143
[13] Qiu L, Jia T M and Yang H J 2016 *Acta Phys. Sin.* **65** 198901 (in Chinese)
[14] Ivanov P C, Liu K K and Bartsch R P 2016 *New J. Phys.* **18** 100201
[15] Zeng J, Zeng C, Xie Q, Guan L, Dong X and Yang F 2016 *Physica A* **462** 1273
[16] Granger C W 1969 *Econometrica* **37** 424
[17] Tang Y, Xiong J J, Luo Y and Zhang Y C 2019 *Int. J. Electron. Commun.* **23** 85
[18] Qiu L and Yang H 2020 *Physica A* **559** 125121
[19] Shannon C E 1948 *The Bell Sys. Tech. J.* **27** 379
[20] Cover T M and Thomas J A 1991 *Elements of information theory*, 2nd ed. (New York: A Wiley-Interscience Publication, John Wiley & Sons, Inc.) p. 12, 019604815.pdf (gbv.de)
[21] Wang Y J, Feng Q Y and Chai L H 2010 *Int. J. Mod. Phys. B* **24** 5949
[22] Mensi W 2012 *Int. J. Manag. Sci. Eng. Manag.* **7** 53
[23] Li X H, Shen X Y and Huang J P 2016 *Chin. Phys. B* **25** 108903
[24] Xu M, Shang P and Huang J 2016 *Commun. Nonlin. Sci. Numer. Simul.* **35** 17
[25] Wang Y and Shang P 2018 *Nonlinear Dyn.* **94** 1361
[26] Wu Y, Shang P and Xia J 2021 *Nonlinear Dyn.* **103** 741
[27] Bentes S R, Menezes R and Mendes D A 2008 *Physica A* **387** 3826
[28] Schreiber T 2000 *Phys. Rev. Lett.* **85** 461
[29] Bossomaier T, Barnett L, Harre M and Lizier J T 2016 *An Introduction to Transfer Entropy: Information Flow in Complex Systems* (SpringerLink (Online service)) p. 65
[30] Mao X and Shang P 2017 *Commun. Nonlinear Sci. Numer. Simul.* **47** 338
[31] Zhou L, Qiu L, Gu C and Yang H 2018 *Europhys. Lett.* **121** 48002
[32] Zheng B, Jiang X F and Ni P Y 2014 *Chin. Phys. B* **23** 078903
[33] Qiu T, Zheng B and Chen G 2010 *New J. Phys.* **12** 043057
[34] Li Y, Jiang X F, Tian Y, Li S P and Zheng B 2019 *Physica A* **515** 671
[35] Shen J and Zheng B 2009 *Europhys. Lett.* **86** 48005
[36] Schmid P and Sesterhenn J 2008 61*st Annual Meeting of the APS Division of Fluid Dynamics*, American Physical Society, November 23–25, 2008, San Antonio, Texas, USA, pp. MR-007
[37] Schmid P J, Meyer K E and Pust O 2009 *Conference proceedings - 8th International Symposium on Particle Image Velocimetry*, August 25–28, 2009, Melbourne, Australia, p. 25, paper2.dvi (oliver-pust.de)
[38] Schmid P J 2010 *J. Fluid Mech.* **656** 5
[39] Schmid P J, Li L, Juniper M P and Pust O 2011 *Theor. Comput. Fluid Dyn.* **25** 249
[40] Hirsh S M, Harris K D, Kutz J N and Brunton B W 2020 *SIAM J. Appl. Dyn. Syst.* **19** 1920
[41] Kutz J N, Brunton S L, Brunton B W and Proctor J L 2016 *Dynamic Mode Decomposition: Data-Driven Modeling of Complex Systems* (SIAM-Society for Industrial and Applied Mathematics) p. 25
[42] Tu J H, Rowley C W, Luchtenburg D M, Brunton S L and Kutz J N 2014 *J. Comput. Dyn.* **1** 391
[43] Brunton S L, Proctor J L and Kutz J N 2016 *Proc. Natl. Acad. Sci. USA* **113** 3932
[44] Heifetz E and Farrell B F 2008 *Q. J. Roy. Meteor. Soc.* **134** 1627
[45] Sujith R I, Juniper M P and Schmid P 2016 *Int. J. Spray Combust.* **8** 119
[46] Nicoletti S, Fanelli D, Zagli N, Asllani M, Battistelli G, Carletti T, Chisci L, Innocenti G and Livi R 2019 *Chaos: Interd. J. Nonlinear Sci.* **29** 083123